Journal of Advanced Research 29 (2021) 191–205

Contents lists available at ScienceDirect

Journal of Advanced Research

journal homepage: www.elsevier.com/locate/jare

A multilayered cross-species analysis of GRAS transcription factors uncovered their functional networks in plant adaptation to the environment

Moyang Liu [a,b,1], Wenjun Sun [a,b,1], Chaorui Li [a], Guolong Yu [a], Jiahao Li [a], Yudong Wang [a], Xu Wang [a,*]

[a] Joint Center for Single Cell Biology, School of Agriculture and Biology, Shanghai Jiao Tong University, Shanghai 200240, China
[b] College of Life Science, Sichuan Agricultural University, Ya'an 625014, China

HIGHLIGHTS

- Polyploidization events were the main driving force for GRASs expansion.
- Evolutionary analysis reveals that inter-species GRASs functions may be conserved.
- GRASs helped plants resist stress by regulating flavonoids pathway.
- GRASs regulate flavonoid synthesis by crosstalk with auxin and photosynthetic pathway.
- Polyploidized GRASs play key roles in environment adaption, growth and development.

GRAPHICAL ABSTRACT

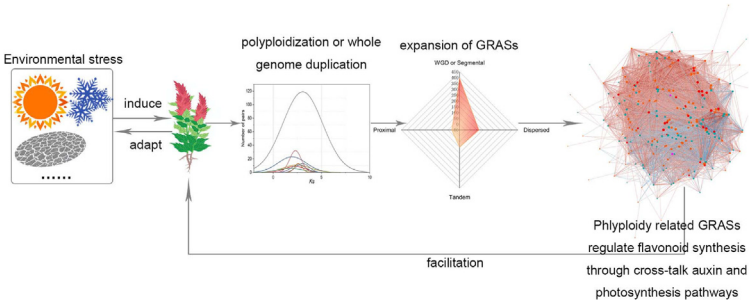

ARTICLE INFO

Article history:
Received 31 August 2020
Revised 7 October 2020
Accepted 24 October 2020
Available online 29 October 2020

Keywords:
GRAS
Environmental stress
Polyploidization
Plant population
Systems biology

ABSTRACT

Introduction: Environmental stress is both a major force of natural selection and a prime factor affecting crop qualities and yields. The impact of the GRAS [gibberellic acid-insensitive (GAI), repressor of GA1–3 mutant (RGA), and scarecrow (SCR)] family on plant development and the potential to resist environmental stress needs much emphasis.
Objectives: This study aims to investigate the evolution, expansion, and adaptive mechanisms of *GRASs* of important representative plants during polyploidization.
Methods: We explored the evolutionary characteristics of *GRASs* in 15 representative plant species by systematic biological analysis of the genome, transcriptome, metabolite, protein complex map and phenotype.
Results: The GRAS family was systematically identified from 15 representative plant species of scientific and agricultural importance. The detection of gene duplication types of *GRASs* in all species showed that the widespread expansion of *GRASs* in these species was mainly contributed by polyploidization events. Evolutionary analysis reveals that most species experience independent genome-wide duplication (WGD) events and that interspecies *GRAS* functions may be broadly conserved. Polyploidy-related *Chenopodium quinoa GRASs* (*CqGRASs*) and *Arabidopsis thaliana GRASs* (*AtGRASs*) formed robust networks with flavonoid pathways by crosstalk with auxin and photosynthetic pathways. Furthermore, *Arabidopsis thaliana* population transcriptomes and the 1000 Plants (OneKP) project confirmed that *GRASs* are components of flavonoid biosynthesis, which enables plants to adapt to the environment by promoting

Peer review under responsibility of Cairo University.
* Corresponding author.
E-mail addresses: cooljeep@sjtu.edu.cn (M. Liu), xu.wang@sjtu.edu.cn (X. Wang).
[1] These authors contributed equally to this work.

https://doi.org/10.1016/j.jare.2020.10.004

flavonoid accumulation. More importantly, the *GRASs* of important species that may potentially improve important agronomic traits were mapped through TAIR and RARGE-II publicly available phenotypic data. Determining protein interactions and target genes contributes to determining *GRAS* functions.
Conclusion: The results of this study suggest that polyploidy-related *GRASs* in multiple species may be a target for improving plant growth, development, and environmental adaptation.

Introduction

Plants live in constantly changing environments that are often adverse to their growth and development [1]. In particular, the frequent occurrence of extreme weather events due to global climate change has made plants more vulnerable to environmental stresses such as salt, abnormal temperatures and drought stress, greatly increasing the vulnerability of agricultural production. How plants perceive stress signals and survive in adverse environments represents fundamental and key biological problems.

Polyploidy, or whole-genome duplication (WGD), is one of the key forces of ecological and evolutionary processes in plants [2]. Caused by abnormal environments, polyploidization, or WGD, can increase the adaptive plasticity of plants to environments and the genetic variability of plants [3]. Polyploidy is particularly common in plants, with all angiosperms sharing ancestral polyploid events and 24% of existing plant species being recent polyploids [2,4]. During evolution and genome diploidization, many duplicated genes have been lost or highly modified, and the number of duplicated chromosomes has been rearranged and reduced, leaving multiple duplicated genes without obvious cytological evidence of WGD [5]. This genetic redundancy caused by WGD allows new functional evolution and functional division between duplicates [6,7], leading to a reduced probability of lineage extinction [8,9]. There is increasing evidence that polyploids exhibit greater resistance to stress compared to diploids under the same genetic background [10,11]. Consequently, polyploidy may promote plant evolvability and improve the adaptability of the population under certain conditions [12]. After polyploidization, genes involved in signal transduction and transcriptional regulation are often expanded, e.g., transcription factor (TF) families, whose evolution and expansion may be related to WGD events [13] and can enhance plant resistance to environmental stress [14].

The GRAS family is named after the three first identified members, including gibberellic acid-insensitive (GAI), repressor of GA1–3 mutant (RGA), and scarecrow (SCR) [15]. As a plant-specific TF family, it plays a pivotal role in multiple signal transduction pathways controlling plant development and stress responses [16,17]. Most GRASs contain a highly conserved C-terminal GRAS domain and a variable N-terminal domain [18]. The GRAS domain is composed of five motifs, including LHRI, VHIID, LHRII, PFYRE, and SAW. In contrast, the N-termini are highly variable and involved mainly in molecular recognition [19,20]. Genome-wide identification of GRAS families has been performed in some species, including *Glycine* max [21], cassava [22], cucumber [23], barley [24], etc. The GRAS family is further divided into different subfamilies, including DELLA, HAM, LS, LISCL, NSP2, PAT1, SCR, SCL3, and SHR, according to different functions [19]. Although static characterization of *GRAS* has been carried out within individual plant genomes, the cross-species evolution of the GRAS family and *GRAS* regulatory network in plant adaptation to environments after polyploidization is still unclear.

A deep understanding of *GRAS* evolution in different plants after polyploidization is indispensable to improving crop quality and environmental adaptability. In addition to *Arabidopsis thaliana*, other plant species have been used as models to study more specific traits or characteristics that do not exist in the model plant. For example, rice has been widely studied as a model plant for species important for human food security, such as wheat, maize, and sorghum. In addition, *Chenopodium quinoa* (quinoa), as a polyploid crop with high nutrition, adapts to many environmental stresses and can thus be used as an ideal model of polyploid plants for *GRAS* research on stress resistance.

To remedy the gap in our knowledge of *GRAS* evolution after polyploidization, some representative plants were selected to explore the adaptive evolution of the *GRAS* regulatory network and to identify important genes in the network related to stress resistance and other agronomic traits. The 15 representative plant species of scientific and agricultural importance include model plants rice and *Arabidopsis thaliana*, a basal angiosperm *Amborella trichopoda*, *Chenopodium quinoa*, *Solanum tuberosum*, *Solanum lycopersicum*, etc. Most species in this study experienced independent WGD events, which further confirmed that the widespread expansion of *GRASs* in these species was associated with polyploidization. Genome synteny and evolutionary rates reveal that the function of *GRASs* may be broadly conserved among *Chenopodium quinoa*, *Arabidopsis thaliana*, *Solanum tuberosum* and *Fagopyrum tataricum*. According to a systematic integration of phenotype, genome, transcriptome, metabolome, and protein interaction data from different plant species and populations, *GRASs* interact with multiple pathways, e.g., auxin signaling and photosynthesis, to regulate flavonoid biosynthesis and plant resistance to various environmental stresses. With these results taken together, this study analyzed the expansion and evolution of *GRASs* and provides a comprehensive dissection of the *GRAS* regulatory network that improves plant adaptation to environments after polyploidization.

Materials and methods

Data sources and sequence retrieval

The genome sequences of the studied species [*Oryza sativa* (diploid) [25], *Arabidopsis thaliana* (diploid) [26], *Fagopyrum tataricum* (diploid) [27], *Beta vulgaris* (diploid) [28], *Chenopodium quinoa* (allotetraploid) [29,30], *Chenopodium pallidicaule* (diploid) [29,31], *Chenopodium suecicum* (diploid) [29], *Daucus carota* (diploid) [32], *Lactuca sativa* (diploid) [33], *Helianthus annuus* (diploid) [34], *Olea europaea* (diploid) [35], *Nicotiana attenuata* (diploid)[36], *Solanum tuberosum* (autotetraploid) [37], *Solanum lycopersicum* (diploid) [38], *Actinidia chinensis* (heterozygous diploid) [39], *Aquilegia coerulea* (diploid) [40] and *Amborella trichopoda* (diploid) [41]] were downloaded from the NCBI.

The public transcriptome data from studies of *A. thaliana* responses to different stimuli, including nutrients [42], mitochondrial stresses [42], chloroplast stresses [42], hormones [auxin (IAA) [43], gibberellin (GA3) [43], abscisic acid (ABA) [43], ethylene (ACC) [43], methyl jasmonate (MEJA) [43], brassinosteroid (BL) [43], zeatin (ZT) [43], and salicylic acid (SA) [44]], abiotic stresses (ozone [45], high light [46], H_2O_2 [44], heat [43], salt [43], UV [43], oxidative [43], and osmotic [43]), and biotic stresses (*Botrytis cinerea* [43], elicitor Flg22 [43], *Erysipheorontii* [43], *Phytophthora*

infestans [43], *Blumeria patens* [47], elicitor EF-Tu [48] and *E. cichoracearum* [49]) were obtained. The transcriptome data for *C. quinoa* includes data from the roots, stems, leaves, flowers, and seeds (GEO: GSE139174). We also obtained proteomics datasets for *A. thaliana*, *O. sativa* and *C. quinoa* [50], as well as the DAP-seq dataset for *A. thaliana* [51]. In addition, transcriptome datasets from 144 natural *A. thaliana* accessions (GEO: GSE43858), the *A. thaliana* 1001 genomes project (GEO: GSE80744) and the 1000 Plants (OneKP) project [52] were obtained.

Genome-wide identification of GRASs

The Hidden Markov Model (HMM) profile of the GRAS domain (PF03514) was downloaded from the Pfam database [53]. The HMM query in the HMMER v3.1 program was used to retrieve all *GRASs* from the 15 genomes with the threshold of an e-value $\leq$ 1e −5 [54] (Table S1, S2). The existence of GRAS domains in all genes identified was validated using HMMER [54], SMART [55], Pfam [56] and InterPro [57].

Identification of GRAS orthogroups in multiple species

The orthogroups of GRAS proteins identified from the 15 species were inferred with OrthoFinder 2 [58], with one copy of the most recent common ancestor of each of these species. Multiple sequence alignment of the *GRAS* proteins in each orthogroup was performed using MUSCLE 3.8.31 [59]. Then, the OrthoFinder 2 results were visualized as a species tree and gene trees with Mega 7 [60]. The orthogroups were divided into LISCL, PAT, HAM, SCL3, SHR, SCR, LAS, DLT, SCL4/7, DELLA, and unclassified subfamilies according to the *A. thaliana* GRAS genes in each orthogroup (Table S2).

Motif composition analyses

The GRAS amino acid sequences from different subfamilies in 15 species were submitted to the Pfam and CDD databases to find other known domains/motifs beyond the GRAS domain. In addition, MEME v4.9.0 [61] was used to identify new conserved motifs not found in public databases (Table S3).

Distribution of GRASs on chromosomes and syntenic and comparative genomics analyses

Chromosome localization information of *CqGRASs*, *AtGRASs*, *FtGRASs* and *StGRASs* was obtained using gff and genome sequence files and visualized through Ciros [62]. The syntenic maps of *A. thaliana*, *F. tataricum*, *C. quinoa*, and *S. tuberosum* were constructed using Dual Synteny Plotter software to identify homologous GRASs within or between these species [63] (Table S4, S6). All proteins or GRASs between *A. thaliana*, *C. quinoa*, *F. tataricum*, and *S. tuberosum* or within each species were analyzed by BLASTP. The syntenic regions within each species and between species were identified by MCscan based on the above BLASTP results [64]. The protein sequences of homologous gene pairs in the identified syntenic region were aligned with MUSCLE and then converted to CDS alignments. The nonsynonymous amino acid substitution rates (Ka) and synonymous amino acid substitution rates (Ks) were calculated using the Ka/Ks calculator [65].

Identification of collinearity and specific duplication events

Gene collinearity analysis was performed using the default parameters in BLAST and MCScanX according to previous studies [66,67]. Different types of duplicated genes were speculated by the duplicate_gene_classifier program in MCScanX, and we inferred collinear genes to identify *GRASs* related to polyploidization. The potential anchoring points (E-value < 1e–5; top five matches) between each possible pair of chromosomes in multiple genomes were found using BLASTP. The loose E-value threshold accommodates the highly differentiated evolution of duplicated genes resulting from polyploidization millions of years ago. Protein sequences were searched against the given genome or genomes of other species. The homologous blocks in each genome or between different genomes were determined with Colinearscan (maximal gap $\leq$ 50 genes; P-value < 0.05) [68]. The maximum gap between neighboring genes along a chromosome showing collinearity with genes along the corresponding chromosome sequence was set as 50 intervening genes [69].

In silico development-related phenotypic analysis

Phenotype data were retrieved from TAIR [70] and RARGE II [71]. The TAIR library contains gain- or loss-of-function phenotypes of *GRAS* mutants in *A. thaliana*. In the RARGEII database, the *GRASs* annotated with increased length, increased size, low saturation, and decreased height were highlighted.

Microarray and RNA-seq data analysis

Raw data from the *A. thaliana* Affymetrix ATH1 array were processed into normalized gene expression values for meta-analysis using RMAExpress v1.1.0. The RNA-seq data were derived from *C. quinoa* leaves, flowers, roots, fruits, and stems. Raw data were processed by FastQC v0.10.1, and the FPKM value of each gene was calculated according to its read count. The hierarchical clustering heatmaps of gene expression were plotted by Tree View software [72].

Gene ontology (GO) annotation

GO analysis was performed using Blast2GO gene ontology analysis tools (http://www.blast2go.com) to determine the molecular functions of differentially expressed genes [73]. GO analysis of target genes bound to *AtGRASs* was performed in the same way.

Network visualization and correlation network construction

The interaction networks of *GRASs* and flavonoid biosynthesis pathway genes, auxin signaling, photosynthesis, and flavonoids under all different stresses were constructed by using the R package imsbInfer in GitHub. The interaction networks in 144 natural *A. thaliana* accessions, the *A. thaliana* 1001 Genomes Project and the 1000 Plants (OneKP) project were constructed in the same way. The associations were calculated using Spearman's rank correlation measure, and the red and blue edges represent positive and negative correlations.

Expressions of differentially expressed CqGRASs in two kinds of C. quinoa fruits

The pale-yellow and dark-yellow *C. quinoa* used in this experiment were grown in a greenhouse at 25℃ and 16 h light/8h dark. The expression patterns of differentially expressed *CqGRASs* in two kinds of *C. quinoa* mature fruits were determined by qRT-PCR (Table S18). The online software primer 3 (http://frodo.wi.mit.edu/) was used to design the primers (Table S18). The gene Elongation Factor 1 alpha (*EF1α*) gene was used as an internal reference gene, and SYBR Premix Ex Taq II (TaKaRa) was used to perform qRT-PCR [74]. The $2^{\triangle\triangle CT}$ method was used to calculate gene expressions [75]. Three technical replicates were performed for each biological replicate, and a total of three biological replicates was set for this experiment.

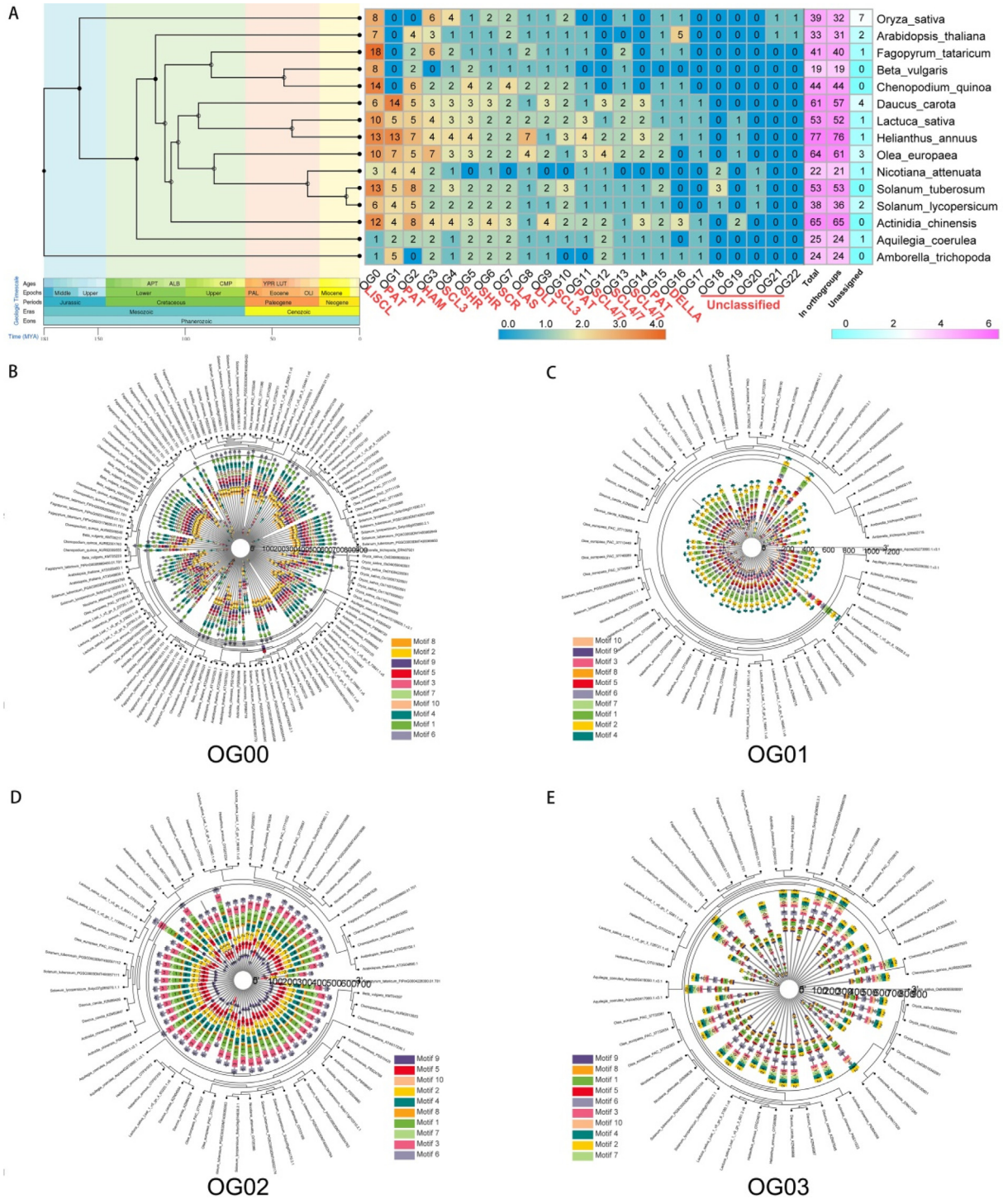

Fig. 1. Phylogeny, diversity and motif compositions of GRAS proteins in 15 species. A. The orthogroups of GRAS proteins identified from the 15 species (*Oryza sativa*, *Arabidopsis thaliana*, *Fagopyrum tataricum*, *Beta vulgaris*, *Chenopodium quinoa*, *Daucus carota*, *Lactuca sativa*, *Helianthus annuus*, *Olea europaea*, *Nicotiana attenuata*, *Solanum tuberosum*, *Solanum lycopersicum*, *Actinidia chinensis*, *Aquilegia coerulea* and *Amborella trichopoda*) were inferred with OrthoFinder 2. Then, the OrthoFinder 2 results were visualized as a species tree with Mega 7. The total number of genes, the numbers of genes in the orthogroups, and the number of unassigned genes are provided. Rows represent the species, and columns represent the orthogroups. The orthogroups were named in turn as different subfamilies, including LISCL, PAT, HAM, SCL3, SHR, SCR, LAS, DLT, SCL4/7, DELLA and unclassified subfamilies, according to the A. thaliana GRAS genes in each orthogroup. B. The phylogenetic relationship of *GRAS* genes of the LISCL subfamily (orthogroup 0) in different species was visualized with Mega 7 (The Outer figure). In addition, MEME v4.9.0 was used to identify conserved motifs of GRASs in 15 species (inner figure). The motifs (numbered 1–10) are displayed in differently colored boxes. The sequence information for each motif is provided in Table S3. C. The phylogenetic relationship of *GRAS* genes of the PAT subfamily (orthogroup 1) in different species was visualized with Mega 7 (Outer figure). In addition, MEME v4.9.0 was used to identify conserved motifs of GRASs in 15 species (inner figure). The motifs (numbered 1–10) are displayed in differently colored boxes. The sequence information for each motif is provided in Table S3. D. The phylogenetic relationship of *GRAS* genes of the PAT subfamily (orthogroup 2) in different species was visualized with Mega 7 (The Outer figure). In addition, MEME v4.9.0 was used to identify conserved motifs of GRASs in 15 species (inner figure). The motifs (numbered 1–10) are displayed in differently colored boxes. The sequence information for each motif is provided in Table S3. E. The phylogenetic relationship of *GRAS* genes of the HAM subfamily (orthogroup 3) in different species was visualized with Mega 7 (Outer figure). In addition, MEME v4.9.0 was used to identify conserved motifs of GRASs in 15 species (inner figure). The motifs (numbered 1–10) are displayed in differently colored boxes. The sequence information for each motif is provided in Table S3.

Statistics

All data were analyzed using the Origin Pro 2020b statistics program, and the means were compared by the least significant difference test at the 0.05 level of significance.

Results

Identification, phylogenetic analysis, motif evolution and expansion of GRASs from representative plants

In total, 658 *GRASs* were identified from 15 representative plant genomes, with copy numbers ranging from 19 to 77 (Fig. 1A, Table S1), and were divided into 22 orthogroups based on their shared primitive ancestral copy genes. The orthogroups were renamed as different subfamilies based on the *AtGRASs* in each orthogroup (Table S2). Orthogroup 0 was renamed the LISCL subfamily, orthogroups 1, 2, 10 and 15 were renamed the PAT subfamily, orthogroups 3 and 11 were renamed the HAM subfamily, orthogroup 4 was renamed the SCL3 subfamily, orthogroups 5 and 6 were renamed the SHR subfamily, orthogroup 7 was renamed the SCR subfamily, orthogroup 8 was renamed the LAS subfamily, orthogroup 9 was renamed the DLT subfamily, orthogroups 12–14 were renamed the SCL4/7 subfamily, orthogroup 16 was renamed the DELLA subfamily, and orthogroups 17–22 were renamed the unclassified subfamily

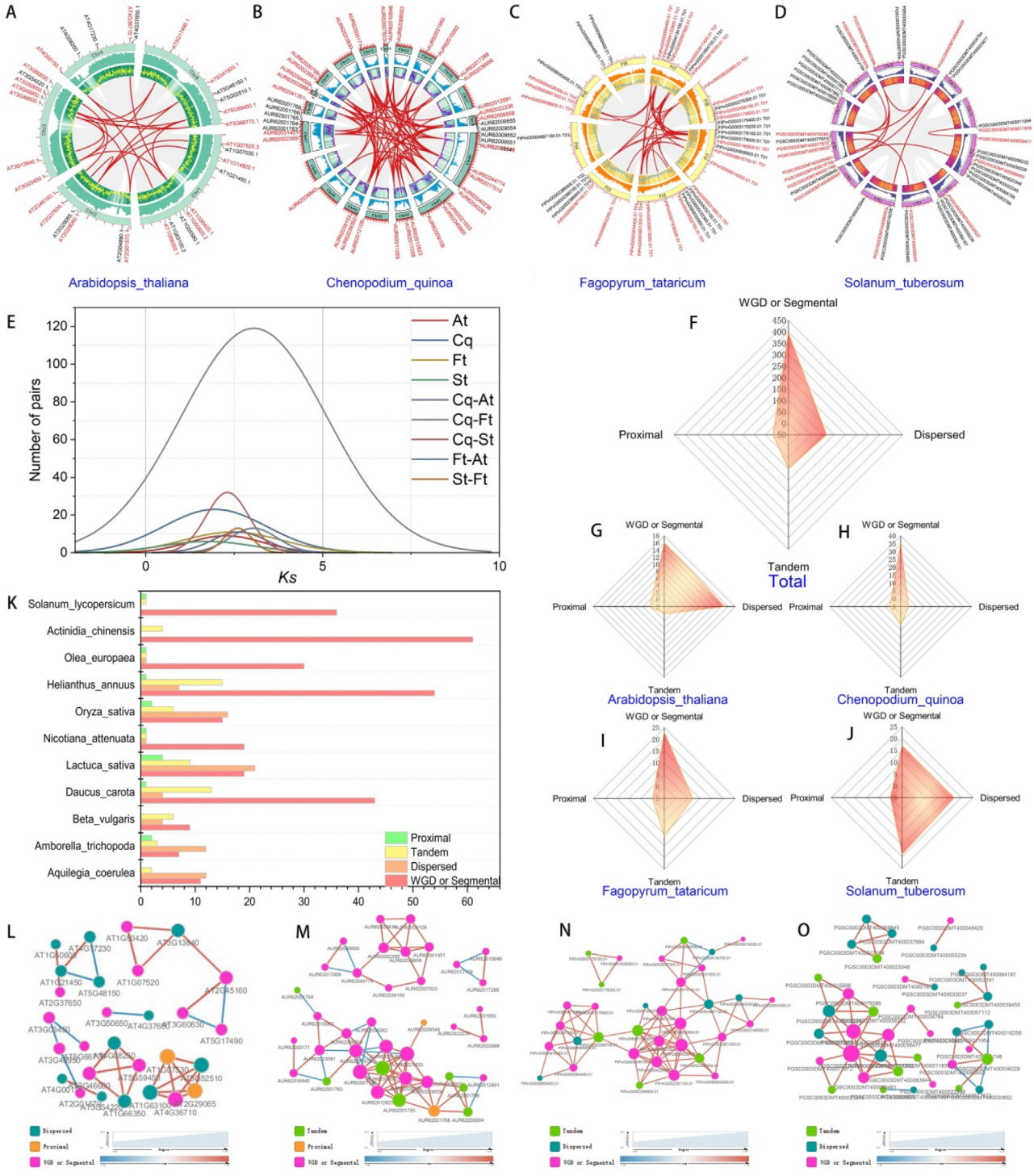

(Fig. 1A). Among most species, LISCL and PAT subfamily members have multiple copies due to their family expansion during evolution, which is in sharp contrast to genes in other groups that exhibit low copy numbers or deletion. The phylogenetic tree based on the alignment of GRAS protein sequences shows that the LISCL subfamily has a more complex topology across multiple species (Fig. 1B).

Further analysis of the existence, origin and evolution of motifs in each subfamily revealed the differences in conserved motif types (Fig. 1B-E). For example, the conserved motifs of LISCL subfamily (orthogroup 0) members are motifs 2, 8 and 9 (Fig. 1B), the conserved motifs of PAT subfamily (orthogroup 1) members are motifs 1, 2 and 4 (Fig. 1C), and the conserved motifs of PAT subfamily (orthogroup 2) members are motifs 1, 2, 3, 5, 6, 7 and 8 (Fig. 1D) (Fig. 1, Table S3). Some ancestral motifs were lost after species differentiation. For instance, in the LISCL subfamily (orthogroup 0), the basal angiosperm *Amborella trichopoda* contained all ten motifs, while *Daucus carota* yielded no detection of motifs 1, 3, 4, 6, 7 or 10, implying that these lost motifs may be replaced by other motifs or that their loss does not affect the execution function of GRASs (Fig. 1).

Polyploidization contributed to the expansion of GRASs in these species

The distribution and collinearity of *GRASs* in different species were analyzed (Fig. 2A-D), and *GRASs* were not evenly distributed on chromosomes in all species, with the number of segmental duplicated *GRASs* in *C. quinoa* being the most abundant (Fig. 2B, Table S4). It is speculated that the differences in the number of *GRASs* among species may be due to gene duplication. The Ks values of homologous pairs in these syntenic regions, as well as the mean Ks values of individual syntenic blocks, indicated that WGD events had occurred in the evolutionary history of these species (Fig. 2E, Table S4). Nevertheless, *C. quinoa* experienced an independent WGD event after differentiation from *A. thaliana*, *F. tataricum* and *S. tuberosum*, which may be an important driving force for the production of homologous *GRAS* in the *C. quinoa* genome (Fig. 2E).

Genome polyploidy provides rich possibilities for new variants, which probably produce polyploidy-related genes in evolutionary processes that face environmental stress. To further identify *GRASs* associated with ancestral polyploidization events (WGD or segmental), the Multiple Collinearity Scan toolkit (MCScanX) can be used to detect gene duplication types (Fig. 2F-J). Here, genes related to polyploidy were inferred according to the collinearity persistence of the region around the selected genes. *GRASs* were divided into four groups, including dispersed, proximal, tandem, and WGD or segmental, and *CqGRASs* were extremely overrepresented in polyploidy-related groups (Fig. 2H, Table S5). Similarly, the *GRAS* types in *A. thaliana*, *F. tataricum* and *S. tuberosum* were inferred (Fig. 2G, I, J), and it was found that most of the *GRASs* in *A. thaliana* were polyploidy-related (16, 48.48%) (Fig. 2G, Table S5), while 56.09% of the *GRASs* in *F. tataricum* were polyploidy-related (Fig. 2I, Table S5). The relationship between *GRASs* accumulation and polyploidization in the other 12 plants was also explored (Fig. 2K, Table S5). Except in *Actinidia chinensis*, *S. tuberosum*, *Aquilegia coerulea*, *Lactuca sativa* and *O. sativa*, polyploidization was the predominant mechanism of *GRASs* formation, accounting for 46.8%-94.73% of these homologues (Fig. 2K, Table S5). These phenomena indicated that whole-genome or segmental duplication plays an indispensable role in *GRASs* expansion, and the widespread expansion of *GRASs* in plants may be related to polyploidization. Further analysis of the correlation network of different types of *GRASs* expression in multiple species revealed that the expression of polyploidy-related *GRASs* was closely related (Fig. 2L-O, Table S4).

Genomic synteny conservation of GRASs in different species and phenotypic analysis of AtGRASs maps to GRASs of other species that can potentially regulate agronomic traits

It is worth investigating whether the function of polyploidy-related *GRASs* in multiple species is similar. Thus, the genome sequences of *C. quinoa*, *A. thaliana*, *S. tuberosum* and *F. tataricum* were compared and identified in multiple syntenic regions, among which *C. quinoa* and *F. tataricum* had the most orthologous pairs (Fig. 3A, Table S6). A correlation network analysis was performed on the expression levels of orthologous *GRASs* of *C. quinoa*, *A. thaliana*, *S. tuberosum* and *F. tataricum* (Fig. 3B, Table S6). Strikingly, the expression of the orthologous *GRAS* pairs of these species is tightly correlated (Fig. 3B, Table S6), and this correlation is in sharp contrast to the absence of such a correlation in a random gene set ($P < 0.05$) (Fig. 3C, Table S6). *C. quinoa* is a hybrid of the ancestral A-genome diploid *C. pallidicaule* and ancestral B-genome diploid *C. suecicum* species [76]. By comparing the genome sequences of *C. quinoa* with those of *C. pallidicaule* or *C. suecicum*, it was found that the number of orthologous *GRAS* pairs between them was the same (Fig. S1, Table S6). Moreover, Ka/Ks analysis of *GRAS* homology genes in these species showed that the GRAS family was conserved and retained in the process of species evolution

Fig. 2. Schematic representations of the interchromosomal relationships of *GRASs*, gene duplication types of *GRASs*, WGD events analyses and correlation network analysis of collinear *GRASs* in different species A. Collinear analysis of *GRAS* genes of *Arabidopsis thaliana*. The red lines indicate the synteny blocks in the *Arabidopsis thaliana* genome. B. Collinear analysis of *GRAS* genes of *Chenopodium quinoa*. The red lines indicate the synteny blocks in the *Chenopodium quinoa* genome. C. Collinear analysis of *GRAS* genes of *Fagopyrum tataricum*. The red lines indicate the synteny blocks in the *Fagopyrum tataricum* genome. D. Collinear analysis of *GRAS* genes of *Solanum tuberosum*. The red lines indicate the synteny blocks in the *Solanum tuberosum* genome. E. The proportion of gene pairs in each plant binned according to Ks values. A high proportion of orthologous gene pairs in plant showed similar rates of synonymous substitutions per synonymous site (Ks), indicative of a whole-genome duplication event. F. Distribution of duplication types of *GRASs* in *Arabidopsis thaliana, Fagopyrum tataricum, Chenopodium quinoa, and Solanum tuberosum*. Multiple Collinearity Scan toolkit (MCScanX) was used to detect duplication types to identify *GRASs* associated with ancestral polyploidization events (WGD or segmental). The *GRASs* related to polyploidy were inferred according to the collinearity persistence of the region around the selected genes. *GRASs* were divided into four groups, including dispersed, proximal, tandem, and WGD or segmental. G. Distribution of duplication types of *GRASs* in *Arabidopsis thaliana.* H. Distribution of duplication types of *GRASs* in *Chenopodium quinoa.* I. Distribution of duplication types of *GRASs* in *Fagopyrum tataricum.* J. Distribution of duplication types of *GRASs* in *Solanum tuberosum.* K. Distribution of duplication types of *GRASs* in multispecies including *Lactuca sativa*, *Aquilegia coerulea*, *Amborella trichopoda*, *Beta vulgaris*, *Daucus carota*, *Nicotiana attenuata*, *Oryza sativa*, *Actinidia chinensis*, *Olea europaea*, *Solanum lycopersicum* and *Helianthus annuus.* Multiple Collinearity Scan toolkit (MCScanX) was used to detect duplication types to identify *GRASs* associated with ancestral polyploidization events (WGD or segmental). The *GRASs* related to polyploidy were inferred according to the collinearity persistence of the region around the selected genes. *GRASs* were divided into four groups, including dispersed, proximal, tandem, and WGD or segmental, L. Correlation network of the expression levels of collinear *GRAS* gene pairs in *Arabidopsis thaliana*. Different colored circles represent different types of *GRASs*. The circle size represents the degree of genes in the correlation network, that is, the larger the circle, the more genes associated with the gene. M. Correlation network of the expression levels of collinear *GRAS* gene pairs in *Chenopodium quinoa*. Different colored circles represent different types of *GRASs*. The circle size represents the degree of genes in the correlation network, that is, the larger the circle, the more genes associated with the gene. N. Correlation network of the expression levels of collinear *GRAS* gene pairs in *Fagopyrum tataricum*. Different colored circles represent different types of *GRASs*. The circle size represents the degree of genes in the correlation network, that is, the larger the circle, the more genes associated with the gene. O. Correlation network of the expression levels of collinear *GRAS* gene pairs in *Solanum tuberosum*. Different colored circles represent different types of *GRASs*. The circle size represents the degree of genes in the correlation network, that is, the larger the circle, the more genes associated with the gene. (For interpretation of the references to color in this figure legend, the reader is referred to the web version of this article.)

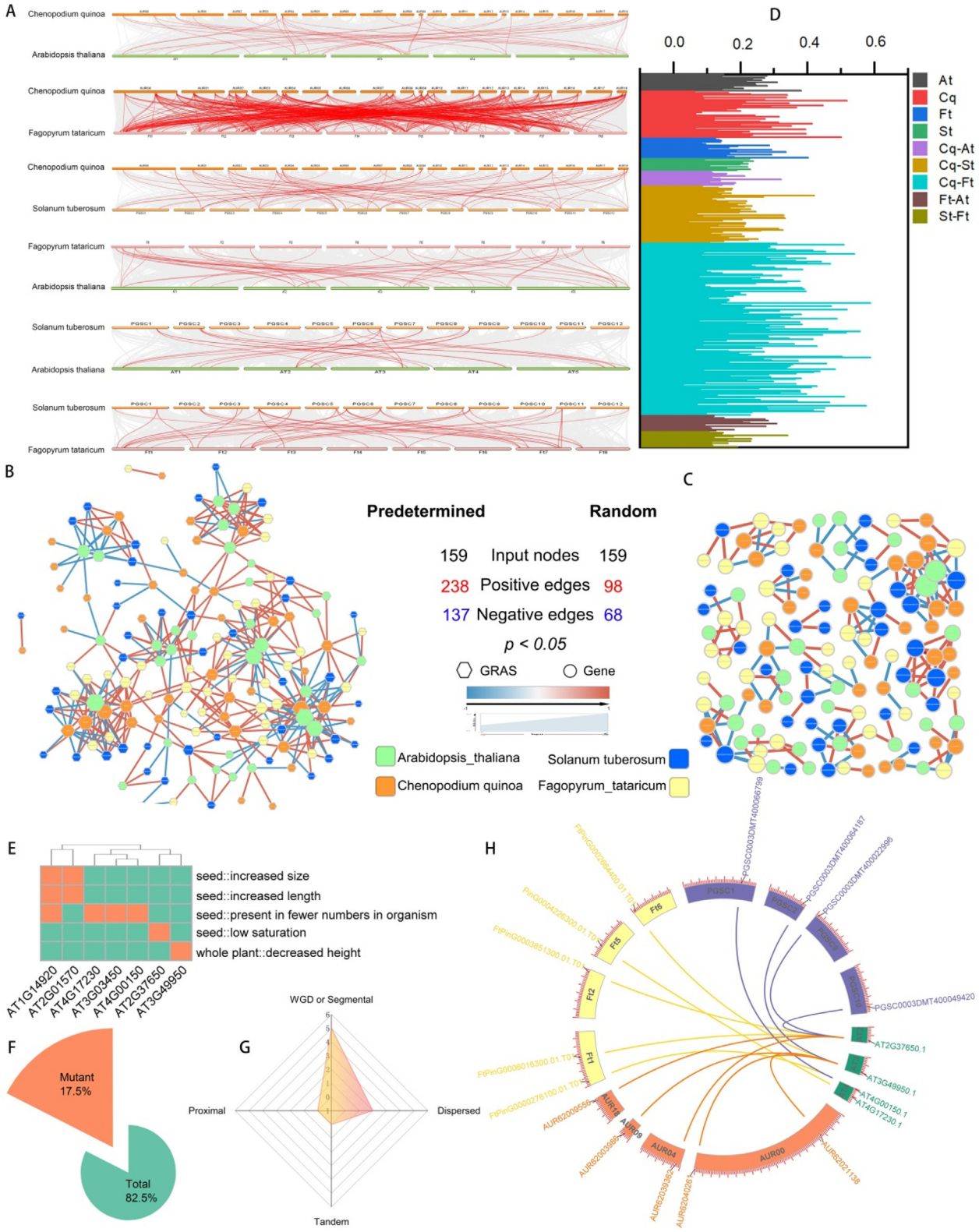

(Fig. 3D). These results indicate that the functions of *GRASs* may be broadly conserved among *C. quinoa*, *A. thaliana*, *S. tuberosum* and *F. tataricum*.

To further explore the potential functions of *GRASs*, publicly available phenotypic data were queried from TAIR and RARGE II to generate a list of 7 *AtGRASs* and the occurrence of mutations that would result in development-related phenotypes (Fig. 3E, F). Six of the *AtGRAS* mutations affected the seed phenotype, while the AT3G49950 mutant decreased the whole plant height (Fig. 3E). It was found that most of the *AtGRASs* were classified as WGD or seg-

mental (Fig. 3G). To further excavate important *GRASs*, these 7 *AtGRASs* were mapped to *CqGRASs*, *FtGRASs* and *StGRASs* with a view toward identifying synteny genes that might perform similar functions (Fig. 3H). *AtGRASs* and *CqGRASs* formed 5 pairs of one-to-many synteny pairs, *AtGRASs* and *FtGRASs* formed 5 pairs of synteny pairs, among which were 3 one-to-one synteny pairs, while *AtGRASs* and *StGRASs* formed 4 pairs of synteny pairs, with 2 one-to-one synteny pairs (Fig. 3H, Table S7). These results mapped some potential development-related candidate genes by identifying *GRASs* of other species with synteny to *AtGRAS* mutants, but the specific functions of these genes need to be confirmed by additional studies.

CF-MS to detect protein interactions and DNA affinity purification sequencing (DAP-seq) mapping genome-wide TF binding sites to jointly determine GRAS functions and phenotypes

Determining protein-protein interactions is another key method by which to analyze gene and protein functions. The interactions between GRASs and other proteins identified by co-fractionation MS (CF-MS) [50] in *A. thaliana*, *O. sativa* and *C. quinoa* revealed 831 conserved protein complexes (Fig. 4A-B, Table S8). Gene ontology (GO) analysis of these conserved proteins interacting with GRASs showed that they are mainly concentrated in the catalytic activity pathways that play an important role in organisms (Fig. 4C-D). By further exploring the interaction network of GRAS proteins in *A. thaliana* (Fig. 4E), it was found that AT2G37650, which affects seed saturation, forms a close network with other proteins (Fig. 3C, Fig. 4F, J). GO analysis of the proteins interacting with AT2G37650 indicated that they were mainly enriched in cellular and metabolic processes and in catalytic activity and binding functions, indicating that they may jointly participate in the regulation of seed saturation (Fig. 4G, Table S10). This interactions were analyzed using transcriptome data from 144 *A. thaliana* accessions (Fig. 4H), which revealed that *AT2G37650* formed a robust network with its directly interacting genes (Fig. 4I, Table S9). Further exploration of their expressions in different tissues showed that the expressions of 16 genes in fruit were similar to that of *AT2G37650*, and these genes could jointly regulate seed saturation (Fig. 4K). The GO analysis of interacting genes with similar expressions of *AT2G37650* indicated that they were mainly enriched in binding terms, which further illustrates their participation in biological processes through protein interaction (Fig. 4L, M).

Interestingly, the interaction networks of GRAS proteins in *C. quinoa* were analyzed (Fig. 4N), indicating that *AUR62009556* and *AUR62039362*, which are homologous to *AT2G37650*, also form a close network with other proteins (Fig. 4O). Furthermore, proteins interacting with *AUR62009556* and *AUR62039362* were also mainly enriched in metabolic processes and binding and catalytic activity functions (Fig. 4P, Table S11). These results suggest that *AUR62009556* and *AUR62039362* may regulate seed saturation by participating in metabolic pathways, and the two genes may have functional redundancy. The interaction networks in two kinds of *C. quinoa* fruits were analyzed, which indicated that only *AUR62039362* formed a robust network with other genes, suggesting that *AUR62039362* might regulate seed phenotype with other genes (Fig. 4Q, Table S12). The interaction gene sets of *AUR62039362* in pale-yellow and dark-yellow *C. quinoa* fruits were also analyzed, and 31 conserved genes interacted with them (Fig. 4R, Table S11). GO analysis of these conserved genes revealed mainly the enrichment of catalytic activity categories, while the category differences in specific interaction sets in two kinds of *C. quinoa* fruits also illustrated the importance of *AUR62039362* and interaction genes in regulating seed saturation (Fig. 4S-U).

Polyploidy-related CqGRASs regulate flavonoid synthesis through auxin and photosynthesis pathway crosstalk

To further verify the functions of the above potential regulators, the transcripts of 44 *CqGRASs* in RNA-seq data from two kinds of *C. quinoa* were analyzed. All *CqGRASs* were hierarchically clustered based on expression in at least one tissue (Fig. 5A). Furthermore, 12 differentially expressed genes (DEGs) in two kinds of *C. quinoa* fruits were identified, including *AUR62039362*, which potentially regulates seed saturation (Fig. 5B). The qRT-PCR results are basically consistent with those of transcriptome analysis, which further confirmed the differential regulatory role of these genes in *C. quinoa* fruits (Fig. S2). The GO enrichment of these DEGs indicated that they have functional differences in protein binding (Fig. 5C). To further explore the function of DEGs, the expressions of differentially expressed proteins bound to *AUR62039362* in pale-yellow and dark-yellow *C. quinoa* fruits were determined (Fig. 5D). Meanwhile, the differential accumulation of anthocyanin, flavonoid and isoflavonol in the pale-yellow and dark-yellow *C. quinoa* fruits was found (Fig. 5E, F, Table S13). It is speculated that differentially expressed *CqGRASs* may interact with other genes to regulate the differential accumulation of metabolites. Furthermore, the directed correlation network of differentially expressed *CqGRASs* with their binding DEGs and differential metabolites was evaluated in *C. quinoa* fruits (Fig. 5G). Strikingly, the expressions of the *CqGRASs* are tightly correlated with their binding genes and metabolite network in *C. quinoa* ($P < 0.05$) (Fig. 5G, Table S14). Meanwhile, *AUR62039362* and its interacting genes and flavonoids, such as rutin, formed a robust directed regulatory network

Fig. 3. Comparative syntenic maps and correlation network of *GRASs* in these representative species and phenotypic analysis of *AtGRASs* maps on to *GRASs* of other species that can potentially regulate agronomic traits A. The synteny relationship of orthologous *GRASs* in *Chenopodium quinoa* and *Arabidopsis thaliana, Chenopodium quinoa* and *Fagopyrum tataricum, Chenopodium quinoa* and *Solanum tuberosum, Fagopyrum tataricum* and *Arabidopsis thaliana, Solanum tuberosum* and *Arabidopsis thaliana, Solanum tuberosum* and *Fagopyrum tataricum*. Gray lines in the background indicate synteny blocks within plant genomes, while red lines highlight syntenic *GRASs* gene pairs. B. The correlation network of the expression levels of syntenic *GRASs* gene pairs of *Arabidopsis thaliana, Fagopyrum tataricum, Chenopodium quinoa, and Solanum tuberosum*. Diamonds represent *GRASs*. Blue diamonds represent *StGRASs*, green diamonds represent *AtGRASs*, dark-yellow diamonds represent *CqGRASs* and pale-yellow diamonds represent *FtGRASs*. The diamonds size represent the degree of genes in the correlation network, that is, the larger the circle, the more genes associated with the gene. C. The correlation network of the expression levels of *GRASs* and random genes of non-syntenic *GRASs*. Circles represent random genes that are not *GRASs*. Blue circles represent random genes of *Solanum tuberosum*, green circles represent random genes of *Arabidopsis thaliana,* dark-yellow circles represent random genes of *Chenopodium quinoa* and pale-yellow circles represent random genes of *Fagopyrum tataricum*. The circles size represent the degree of genes in the correlation network, that is, the larger the circle, the more genes associated with the gene. D. The Ka/Ks ratios represent the evolution rate of *GRAS* genes. Different colored lines represent the Ka/Ks ratios of homologous *GRAS* gene pairs within or between different species. The Ka/Ks ratios less than 1 indicates that the genes have undergone purification selection. E. 7 Arabidopsis GRAS gene mutations will lead to different phenotypic changes. Clustering of 7 *GRASs* according to the type of plant phenotype change after mutation. Orange squares indicate corresponding phenotypic changes after the mutation. F. The proportion of *GRAS* mutants to all *GRAS* genes in *Arabidopsis thaliana*. G. The distribution of gene duplication types of *AtGRASs* and *CqGRASs*. Gene types of *GRAS* mutant genes in *Arabidopsis thaliana*. Multiple Collinearity Scan toolkit (MCScanX) was used to detect duplication types to identify *GRASs* associated with ancestral polyploidization events (WGD or segmental). The *GRASs* related to polyploidy were inferred according to the collinearity persistence of the region around the selected genes. *GRASs* were divided into four groups, including dispersed, proximal, tandem, and WGD or segmental, H. The collinearity between *AtGRASs* with altered phenotypes after mutation and *GRAS* genes of *Arabidopsis thaliana, Fagopyrum tataricum, Chenopodium quinoa, and Solanum tuberosum*. The orange line represents the collinear gene pairs formed by *AtGRASs* and *CqGRASs*. The purple line represents the collinear gene pair formed by *AtGRASs* and *StGRASs*. The yellow lines represent collinearity gene pairs formed by *AtGRASs* and *FtGRASs*. (For interpretation of the references to color in this figure legend, the reader is referred to the web version of this article.)

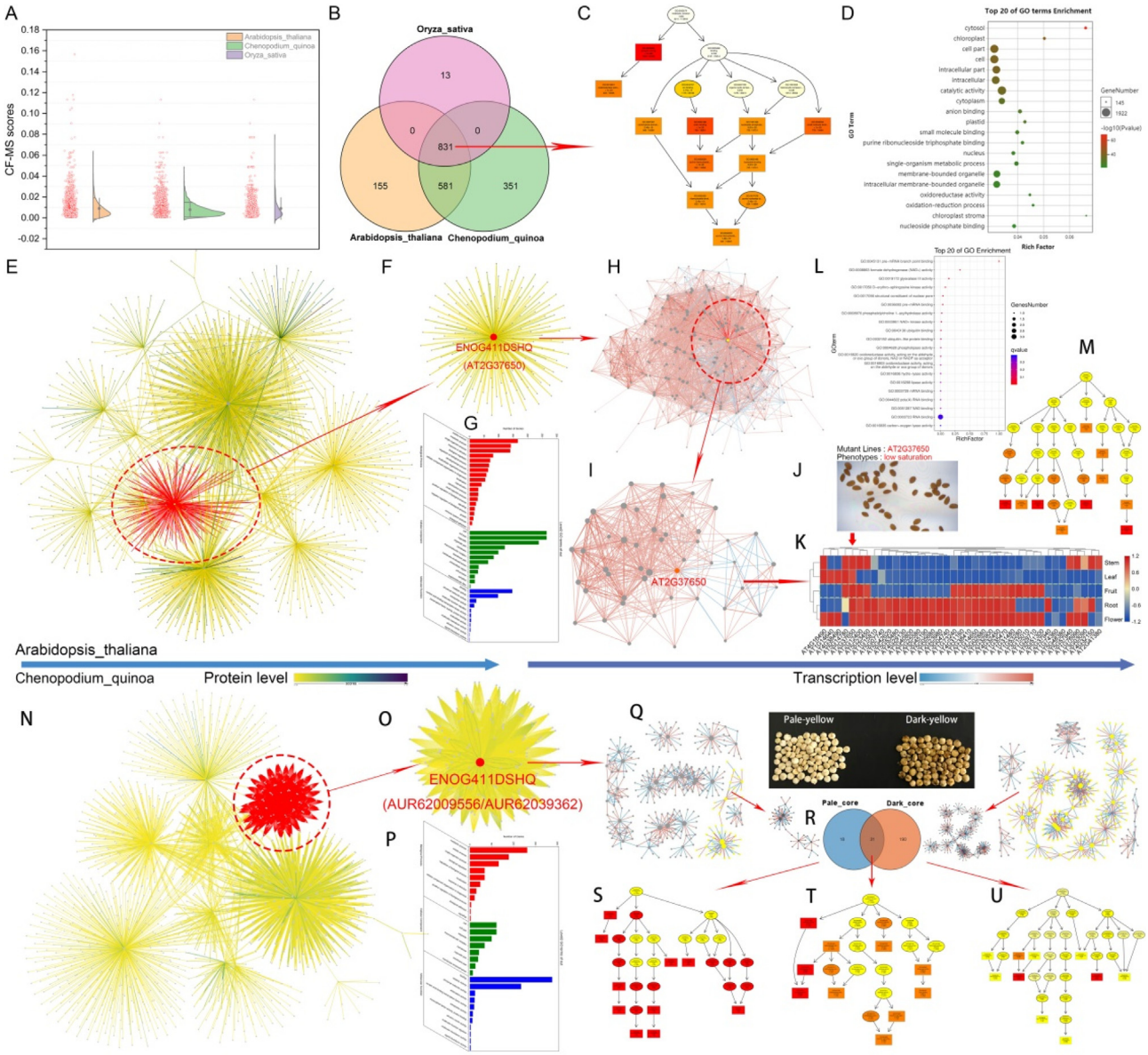

Fig. 4. Co-fractionation MS detects protein interactions and DNA affinity purification sequencing (DAP-seq) mapping genome-wide TF binding sites A. Detection of GRAS protein interacting orthogroups in Arabidopsis, rice and quinoa by Co-fractionation MS. Orange represents Arabidopsis, green represents quinoa, and purple represents rice. The red bubbles represent the orthogroups of proteins interacting with GRASs. B. Venn diagram of the orthogroups of proteins interacting with GRASs in rice, Arabidopsis, and quinoa. The intersection represents a conserved orthogroup of proteins interacting with GRAS proteins in Arabidopsis, rice and quinoa. C. Molecular function analysis of conserved orthogroup of proteins interacting with GRAS proteins in Arabidopsis, rice and quinoa. The color of the graph represents the enrichment degree of interacting proteins with GRASs in GO term. The deeper the color is, the more significant the enrichment is. D. GO enrichment analysis of conserved orthogroup of proteins interacting with GRAS proteins in Arabidopsis, rice and quinoa. Bubble size represents the amount of proteins that interact with GRASs in GO term, and the larger the bubble, the more proteins that interact with GRASs. E. Interaction network between AtGRAS proteins and its interacting proteins in Arabidopsis thaliana. F. At2g37650 mutation will affect seed saturation. The red dotted circle represents an interaction network between AT2G37650 and other proteins. G. The GO analysis of the proteins interacting with AT2G37650. H. This interaction of Arabidopsis ENOG411DSHQ orthogroup was analyzed using transcriptome data from 144 Arabidopsis accessions. I. The red dotted circle represents a robust interaction network between AT2G37650 and its directly interacting genes analyzed using transcriptome data from 144 Arabidopsis accessions. J. Phenotypic changes induced by AT2G37650 mutation. K. Expression levels of genes interacting with AT2G37650 in roots, stems, flowers, leaves and fruits. The closer it is to red, the higher the level of gene expression. L. The genes with similar expression as *AT2G37650* in fruits were regarded as concerned genes. This figure shows the GO analysis of genes interacting with concerned genes. Bubble size represents the amount of proteins that interact with concerned genes in GO term, and the larger the bubble, the more proteins that interact with concerned genes. M. The genes with similar expression as *AT2G37650* in fruits were regarded as concerned genes. This figure shows the molecular function analysis of genes interacting with concerned genes. The color of the graph represents the enrichment degree of interacting proteins with concerned genes in GO term. The deeper the color is, the more significant the enrichment is. N. Interaction network between CqGRAS proteins and its interacting proteins in quinoa. O. The red dotted circle represents an interaction network between the CqGRAS proteins homologous to AT2G37650 and other proteins. P. GO annotation analysis of proteins interacting with AUR62009556 and AUR62039362. Q. Correlation analysis between *AUR62039362* and interaction gene sets in pale-yellow and dark-yellow *C. quinoa* fruits R. Venn diagram of the orthogroups of proteins interacting with *AUR62039362* in pale-yellow and dark-yellow *C. quinoa* fruits. The intersection represents a conserved orthogroup of proteins interacting with *AUR62039362* in pale-yellow and dark-yellow *C. quinoa* fruits. S. Molecular function analysis of proteins interacting with *AUR62039362* in pale-yellow quinoa specific region. T. Molecular function analysis of proteins interacting with *AUR62039362* in two kinds of quinoa common region U. Molecular function analysis of proteins interacting with *AUR62039362* in dark-yellow quinoa specific region. (For interpretation of the references to color in this figure legend, the reader is referred to the web version of this article.)

(P < 0.05) (Fig. 5H, Table S14). The core genes interacting with *AUR62039362* were mainly enriched in metabolic process and phosphotransferase activity terms (Fig. 5I, J).

The above differentially expressed *GRASs* include PAT subfamily members involved in phytochrome-mediated light signal transduction and plant defense [77], LISCL subfamily members involved in auxin and stress-induced signals [19], and SHR subfamily members that regulate root development [78] (Fig. 5B). This leads us to speculate whether the differentially expressed *GRASs* might crosstalk with these pathways to regulate flavonoid synthesis. The correlation networks based on the expression of these *GRASs* and the auxin pathway, photosynthesis, flavonoid biosynthesis pathway genes and metabolites in pale-yellow and dark-yellow *C. quinoa* were further constructed (Fig. 5K, M), and these *GRASs* were closely related with these pathways in both *C. quinoa* types (Fig. 5L, N, Table S15). It was further found that there are two conserved genes

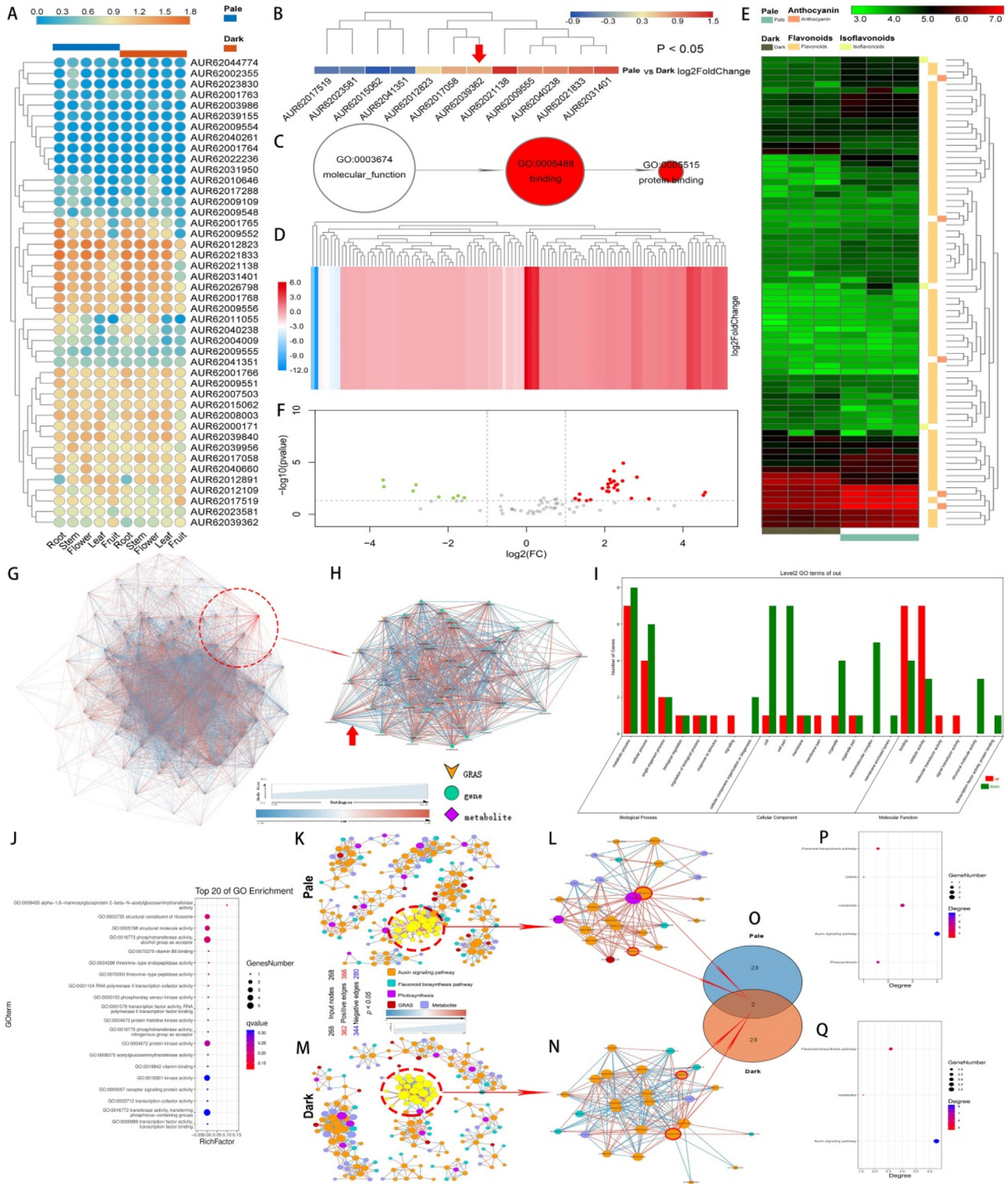

in the most robust correlation network of the two kinds of *C. quinoa*, which interact most closely with other genes (Fig. 5O, Table S15). The degree analysis of the close correlation network found that *GRASs*, photosynthesis, auxin and flavonoid biosynthesis pathways together regulate metabolite synthesis in pale-yellow *C. quinoa* (Fig. 5P), which is in sharp contrast to the absence of *GRASs* and photosynthesis in the close correlation network of dark-yellow *C. quinoa* (Fig. 5Q). The differential flavonoid biosynthesis pathway regulatory network may reveal the differential performance of the two kinds of *C. quinoa* responses to the environment.

Universal applicability correlation network of GRASs, photosynthesis, auxin and flavonoid biosynthesis pathways

In *A. thaliana*, the universality of the correlation network of *GRAS*, photosynthesis, auxin and flavonoid biosynthesis pathway genes was further validated. The correlation network between *AtGRASs* and photosynthesis, auxin and flavonoid biosynthesis pathway genes under different conditions was further validated (Fig. 6A, Table S17). Notably, the expression of *AtGRASs* is tightly correlated with photosynthesis, auxin and flavonoid biosynthesis pathway genes under all environmental stresses, and interaction networks under abiotic stress were more enriched compared to those under other stresses ($P < 0.05$) (Fig. 6A). Meanwhile, most *AtGRAS*, photosynthesis, auxin and flavonoid biosynthesis pathway genes were induced under nearly all abiotic stress conditions, indicating that they were extensively involved in responses to environmental stress (Fig. 6B, Table S16).

To explore the widespread nature of the network, a correlation network analysis of the expression levels of *AtGRASs* and photosynthesis, auxin and flavonoid biosynthesis pathway genes across 144 natural *A. thaliana* accessions [79] was performed (Fig. 6C). Notably, the expression of *AtGRASs* is closely related to the photosynthesis, auxin and flavonoid biosynthesis pathway gene network (Fig. 6C, Table S17), which is in sharp contrast to the absence of such a correlation in a random gene set ($P < 0.01$) (Fig. 6D, Table S17). The *A. thaliana* 1001 Genomes Project (GEO: GSE80744) (Fig. 6E, F, Table S17) and 1000 Plants (OneKP) project [52] also validated this network ($P < 0.01$) (Fig. 6G, H, Table S17), suggesting that *GRASs* may regulate plant growth and development by participating in cross-talk among multiple pathways.

Discussion

GRASs play a central regulatory role in plant growth, development, and stress responses [80,81]. They are therefore promising targets for improved crop breeding. Here, 658 *GRASs* were identified from 15 species and divided into 22 orthogroups. The heterotetraploid nature of *C. quinoa* and the large scale of the GRAS family provide an ideal opportunity to explore the evolution of genes after gene duplication and polyploidization. WGD have events occurred in most species—particularly, *C. quinoa*, *A. thaliana*, *S. tuberosum* and *F. tataricum*—through independent WGD events (Fig. 2F). The evolution of *GRASs* after polyploidization was explored, which indicated that the widespread expansion of *GRASs* in most species is related to polyploidization, and these polyploidy-related *GRASs* may contribute to plant development and adaptation to environmental stress. The high number of GRASs observed in *C. quinoa*, *A. thaliana*, and *F. tataricum* is mainly a result of the significant expansion of the LISCL subfamily. This is consistent with reports on other species [82]. The expansion of the GRAS family is limited to a few subfamilies, and the number of *GRASs* in most subfamilies is constant. Moreover, several subfamilies lack members in one or more species. The absence of representative common orthogroups in closely related species suggests that the loss predated the origin of some subfamilies. In particular, there was a lower number of 19 *GRASs* in *B. vulgaris*, and members of 13 orthogroups were missing (Fig. 1). In a similar study of other transcription factors, no complete loss of subfamily members in a given species was found [83]. Notably, most subfamilies missing members of one or more species belong to subfamilies containing multiple orthogroups [82]. In the unclassified subfamily, most species of multiple orthogroups lack *GRASs*, which suggests that these species may have lost subfamilies that are not important for their growth and development during evolution. The lack of members of some species in these orthogroups indicates that despite their ancient differentiation, the members of the GRAS family of close orthogroups remain redundant to a certain extent, and the complete loss of representative orthogroups in a given species seems to be compensated by the presence of members of the close orthogroups.

Previous studies have identified the GRAS family in a single or several species but have not systematically explored the evolutionary mechanisms of plant *GRASs* after polyploidization [84–86]. By exploring the genomic collinearity among different species, it was found that the functions of polyploid-related *GRASs* in some plants were more conserved. Furthermore, the evolution rates of different species showed that the functions of these genes were relatively conserved. The higher evolution rate of homologous genes in *C. quinoa* suggested that *CqGRASs* might be more conducive to adapting to environmental changes. As plants grow in changing environments, crosstalk between pathways is an absolute requirement for robust growth. Studies have shown that there is crosstalk between different signaling pathways or between hor-

Fig. 5. Polyploidy-related *CqGRASs* developed robust networks with flavonoid biosynthesis pathway genes by crosstalk of auxin signaling and photosynthesis pathway A. Cluster analysis of *CqGRASs* transcripts in roots, stems, leaves, flowers and fruits. B. The differentially expressed *CqGRASs* in two kinds of quinoa fruits. Among these differentially expressed genes, *AUR62017519, AUR62015062, AUR62012823, AUR62017058, AUR62021138, AUR62021833* and *AUR62031401* are PAT subfamily members. *AUR62041351, AUR62039362* and *AUR62009555* are LISCL Subfamily members. *AUR62040238* is SHR subfamily members, and *AUR62023581* is SCL4/7 subfamily members. C. The GO analysis of differentially expressed *CqGRASs* in two kinds of quinoa fruits. D. The expression levels of differential expression proteins bound to *AUR62039362* in two kinds of quinoa fruits. E. Different metabolites (anthocyanin, flavonoid and isoflavonol) in two kinds of quinoa fruits. F. The differencial accumulation of anthocyanin, flavonoid and isoflavonol in the pale-yellow and dark-yellow *C. quinoa* fruits G. The directed correlation network of differentially expressed *CqGRASs* with their binding DEGs and differential metabolites in two kinds of *C. quinoa* fruits. H. The red dotted circle represents the directed interaction network formed by *AUR62039362* and its interacting genes and flavonoids such as rutin. I. The GO annotation of the core genes interacting with AUR62039362 J. The GO enrichment of the core genes interacting with AUR62039362 K. The correlation network of differentially expressed GRASs and auxin pathway, photosynthesis, flavonoid biosynthesis pathway and metabolite in pale-yellow quinoa fruits L. The red dotted circle represents the correlation network with maximum degree of differentially expressed GRASs and auxin pathway, photosynthesis, flavonoid biosynthesis pathway and metabolite formed in pale-yellow quinoa fruits. M. The correlation network of differentially expressed GRASs and auxin pathway, photosynthesis, flavonoid biosynthesis pathway and metabolite in dark-yellow quinoa fruits N. The red dotted circle represents the correlation network with maximum degree of differentially expressed GRASs and auxin pathway, photosynthesis, flavonoid biosynthesis pathway and metabolite formed in dark-yellow quinoa fruits. O. Venn diagram of correlation networks with maximum degree of differentially expressed GRASs and auxin pathway, photosynthesis, flavonoid biosynthesis pathway and metabolite formed in two kinds of quinoa fruits. The intersection represents two conserved genes in the most robust correlation network of two kinds of quinoa fruits, which interact most closely with other genes. P. Degree analysis of the close correlation network of differentially expressed GRASs and auxin pathway, photosynthesis, flavonoid biosynthesis pathway and metabolite formed in pale-yellow quinoa fruits Q. Degree analysis of the close correlation network of differentially expressed GRASs and auxin pathway, photosynthesis, flavonoid biosynthesis pathway and metabolite formed in dark-yellow quinoa fruits. (For interpretation of the references to color in this figure legend, the reader is referred to the web version of this article.)

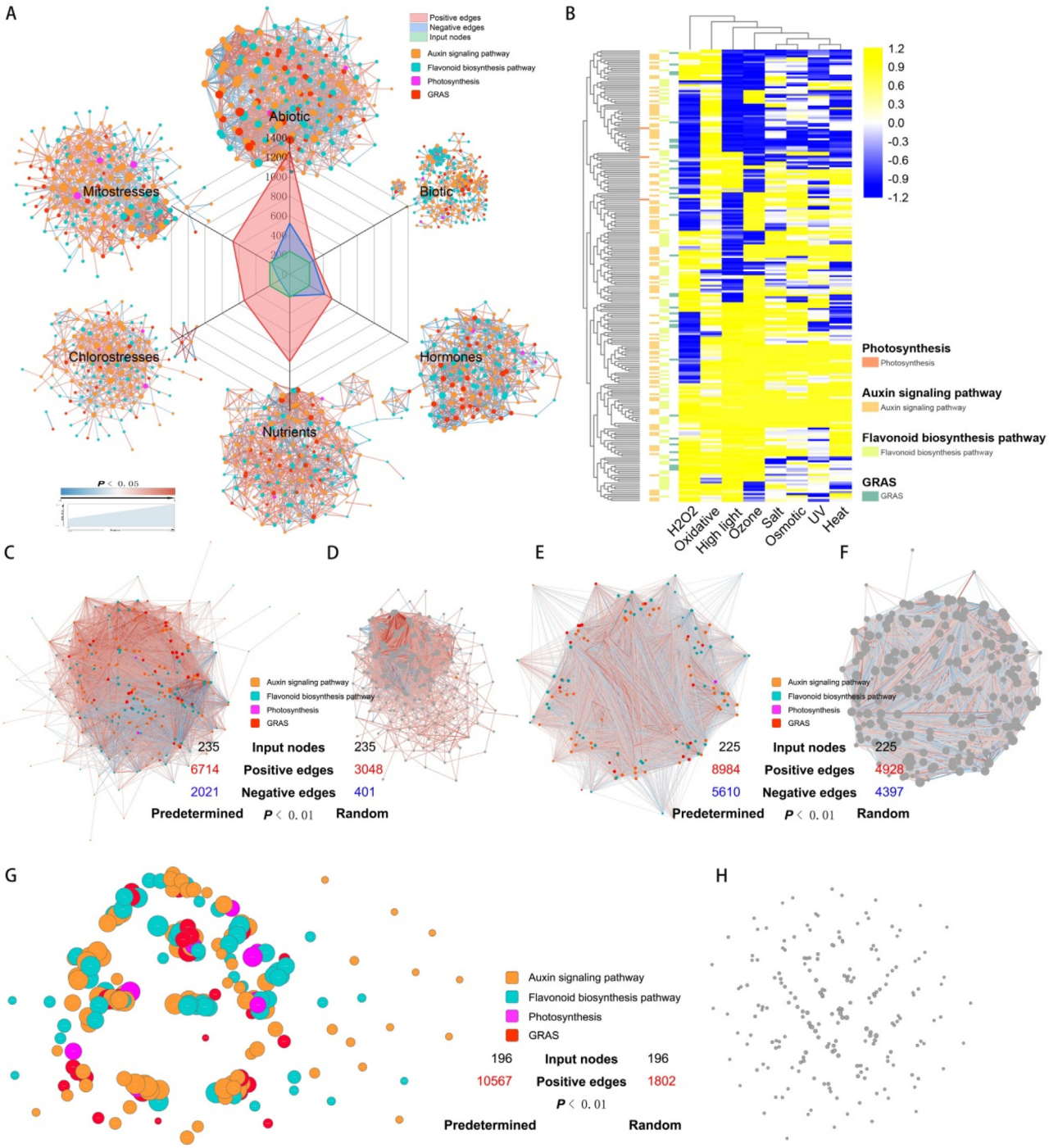

mones and developmental pathways [87–89]. Light signaling plays a critical regulatory role in plant morphogenesis, metabolism, growth and development, and the core process of the light signaling pathway is to establish the relationship between light signaling and related gene expressions [90]. Flavonoids play important roles in a variety of physiological processes [91], and the accumulation of flavonoids in plant tissues depends on the availability of light signals, but the potential regulatory network of light signals controlling flavonoid biosynthesis is rarely known. The biosynthetic process of flavonoids is complex and usually activated by a variety of flavonoid biosynthetic genes, including early biosynthetic genes [92], while flavonoid biosynthesis is also affected by various plant hormones, such as auxin [93], methyl jasmonate [94,95], salicylic acid [94,95], etc. Both the light signaling pathway and the auxin pathway play pivotal roles in regulating flavonoid synthesis. As a positive regulator, AtPAT1 from the PAT subfamily participates in the phytochrome A (phy A)-specific signaling pathway and plays an important role in the early stage of the phy A signaling cascade [77]. Moreover, LISCL subfamily members are reported to play important regulatory roles in auxin signaling [19]. The differentially expressed *GRASs* identified in two kinds of *C. quinoa* fruits belong to the LISCL and PAT subfamilies, which raised an interesting question concerning whether these GRASs might regulate flavonoid synthesis by cross-talk between these pathways.

Fig. 6. *AtGRASs* developed robust networks with flavonoid biosynthesis pathway genes by crosstalk of auxin signaling and photosynthesis pathway under various environmental stresses A. *AtGRASs* developed robust networks with flavonoid biosynthesis pathway genes by crosstalk of auxin signaling and photosynthesis pathway under various environmental stresses. Auxin signaling pathway genes are represented by orange circles, flavonoid biosynthesis pathway genes are represented by light blue circles, photosynthesis pathway genes are represented by pink circles, and *AtGRAS* genes are represented by red circles. The circle size represents the degree of genes in the correlation network, that is, the larger the circle, the more genes associated with the gene. B. Expression of *AtGRASs* and auxin signaling, photosynthesis pathway and key flavonoid genes under abiotic stress treatments. C. Correlation network analysis of the expression levels of *AtGRASs* and auxin signaling, photosynthesis pathway and key flavonoid genes in 144 natural *Arabidopsis* accessions. Auxin signaling pathway genes are represented by orange circles, flavonoid biosynthesis pathway genes are represented by light blue circles, photosynthesis pathway genes are represented by pink circles, and *AtGRAS* genes are represented by red circles. The circle size represents the degree of genes in the correlation network, that is, the larger the circle, the more genes associated with the gene. D. Correlation network analysis of the expression levels of *AtGRASs* and random genes in 144 natural *Arabidopsis* accessions. *AtGRAS* genes are represented by red circles, and random genes are represented by grey circles. The circle size represents the degree of genes in the correlation network, that is, the larger the circle, the more genes associated with the gene. E. Correlation network analysis of the expression levels of *AtGRASs* and auxin signaling, photosynthesis pathway and key flavonoid genes in Arabidopsis 1001 Genomes Project. Auxin signaling pathway genes are represented by orange circles, flavonoid biosynthesis pathway genes are represented by light blue circles, photosynthesis pathway genes are represented by pink circles, and *AtGRAS* genes are represented by red circles. The circle size represents the degree of genes in the correlation network, that is, the larger the circle, the more genes associated with the gene. F. Correlation network analysis of the expression levels of *AtGRASs* and random genes in Arabidopsis 1001 Genomes Project. *AtGRAS* genes are represented by red circles, and random genes are represented by grey circles. The circle size represents the degree of genes in the correlation network, that is, the larger the circle, the more genes associated with the gene. G. Correlation network analysis of the expression levels of *AtGRASs* and auxin signaling, photosynthesis pathway and key flavonoid genes in 1000 Plants (OneKP) project. Auxin signaling pathway genes are represented by orange circles, flavonoid biosynthesis pathway genes are represented by light blue circles, photosynthesis pathway genes are represented by pink circles, and *AtGRAS* genes are represented by red circles. The circle size represents the degree of genes in the correlation network, that is, the larger the circle, the more genes associated with the gene. H. Correlation network analysis of the expression levels of *AtGRASs* and random genes in 1000 Plants (OneKP) project. *AtGRAS* genes are represented by red circles, and random genes are represented by grey circles. The circle size represents the degree of genes in the correlation network, that is, the larger the circle, the more genes associated with the gene. (For interpretation of the references to color in this figure legend, the reader is referred to the web version of this article.)

This study identified differentially expressed *GRASs*, which, in combination with other interacting genes, result in differences in the flavonoid contents of two kinds of *C. quinoa* fruits (Fig. 5). Furthermore, a correlation network of differentially expressed *GRASs* with the light signaling pathway, auxin signaling pathway and flavonoid biosynthesis pathway was constructed, which confirmed that *GRASs* can regulate flavonoid synthesis by crosstalk between multiple pathways. Interestingly, *GRASs* in *A. thaliana* can regulate the synthesis of flavonoids by crosstalk between multiple pathways under various environmental stresses. Meanwhile, *GRASs* have formed a robust correlation network with these pathways in *A. thaliana* populations and 1000 plants, which confirms that *GRASs*, as a core component, may regulate the synthesis of plant flavonoids through multiple cross-talk pathways. These in-depth studies will identify and confirm interactions and further clarify the role of interactions in molecular networks and biological processes. Nevertheless, despite our growing understanding of the role of TFs in these processes, the transcriptional regulation of genes and their complex qualitative and quantitative cooperativity between proteins and DNA remain to be investigated.

Conclusions

Our work not only provides a panoramic view of the evolution and expansion of *GRASs* in important species but also provides the first step for more detailed investigations of the functional diversity of *GRASs* of important nutritional crops after polyploidization. Our data highlight the universality of the robust correlation network between polyploid-related *GRASs* achieved by crosstalk between multiple pathways and flavonoid pathways. Furthermore, the population transcriptome emphasizes the universality of the key features of polyploidy-related *GRASs* in the flavonoid synthesis pathway, which is a role implying that they regulate plant metabolism by being involved in multiple pathways to achieve plant environmental adaptation. The interactive proteins that we identified may share functions, and although further identification of *GRAS* roles is required, information on their stable interaction with other proteins or genes will guide future research. Comprehensive and systematic analysis of the regulatory network of *GRAS* adaptation to the environment after polyploidization through multiomics and phenotype may contribute to understanding the gene expansion mechanisms of important crops under polyploidy and provide valuable resources for important crop breeding.

Compliance with ethics requirements

This article does not contain any studies with human or animal subjects.

Author Contributions

M.-Y.L. planned and designed the research. M.-Y.L., C.-R.L., J.-H. L. and G.-L.Y. performed the experiments and analyzed the results. W.-J.S. and X.W. wrote the original manuscript. W.-J.S. and Y.-D.W. revised the manuscript. M.-Y.L. and X.W. supervised the research. All authors read and approved the final manuscript.

Declaration of Competing Interest

The authors have declared no conflict of interest.

Acknowledgements

This research was sponsored by National Natural Science Foundation of China (32071160), Shanghai Pujiang Program (19PJ1406600), Shanghai Sailing Program (20YF1422000), Natural Science Foundation of Shanghai (20ZR1427900) and the Shanghai Jiao Tong University (WF220415005 & 20X100040052).

Appendix A. Supplementary material

Supplementary data to this article can be found online at https://doi.org/10.1016/j.jare.2020.10.004.

References

[1] Zhu J-K. Abiotic stress signaling and responses in plants. Cell 2016;167:313–24.
[2] Forrester N, Rebolleda-Gómez M, Sachs J, Ashman T-L. Polyploid plants obtain greater fitness benefits from a nutrient acquisition mutualism. New Phytol 2020;227.
[3] Van de Peer Y, Mizrachi E, Marchal K. The evolutionary significance of polyploidy. Nat Rev Genet 2017;18.
[4] Barker M, Arrigo N, Baniaga A, Li Z, Levin D. On the relative abundance of autopolyploids and allopolyploids. New Phytologist 2015;210.
[5] Feliner G, Casacuberta J, Wendel J. Genomics of evolutionary novelty in hybrids and polyploids. Front Genet 2020;11.
[6] Freeling M, Scanlon M, Fowler J. Fractionation and subfunctionalization following genome duplications: Mechanisms that drive gene content and their consequences. Curr Opin Genet Dev 2015;35:110–8.

[7] Conant G, Birchler J, Pires J. Dosage, duplication, and diploidization: Clarifying the interplay of multiple models for duplicate gene evolution over time. Curr Opin Plant Biol 2014;19C:91–8.
[8] Donoghue P, Purnell M. Genome duplication, extinction and vertebrate evolution. Trends Ecol Evol 2005;20:312–9.
[9] Fawcett J, Maere S, Van de Peer Y. Plants with double genomes might have had a better chance to survive the Cretaceous-Tertiary extinction event. Proc Nat Acad Sci United States America 2009;106:5737–42.
[10] Allario T, Brumos J, Colmenero J, Iglesias D, Pina J, Navarro L, et al. Tetraploid Rangpur lime rootstock increases drought tolerance via enhanced constitutive root ABA production. Plant, Cell Environ 2012;36.
[11] Chao D-Y, Dilkes B, Luo H, Douglas A, Yakubova E, Lahner B, et al. Polyploids exhibit higher potassium uptake and salinity tolerance in arabidopsis. Science (New York, N.Y.) 2013;341.
[12] Shi X, Zhang C, Ko DK, Chen ZJ. Genome-wide dosage-dependent and -independent regulation contributes to gene expression and evolutionary novelty in plant polyploids. Mol Biol Evol 2015;32:2351–66.
[13] Lehti-Shiu M, Panchy N, Wang P, Uygun S, Shiu S-H. Diversity, expansion, and evolutionary novelty of plant DNA-binding transcription factor families. Biochim Biophys Acta (BBA) - Gene Regulatory Mech 2016;1860.
[14] Wang N, Yang Y, Moore M, Brockington S, Walker J, Brown J, et al. Evolution of portulacineae marked by gene tree conflict and gene family expansion associated with adaptation to harsh environments. Mol Biol Evol 2018.
[15] Pysh L, Diller J, Camilleri C, Bouchez D, Benfey P. The GRAS gene family in Arabidopsis: sequence characterization and basic expression analysis of the SCARECROW-LIKE genes. Plant J: Cell Mol Biol 1999;18:111–9.
[16] Guo P, Wen J, Yang J, Ke Y, Wang M, Liu M, et al. Genome-wide survey and expression analyses of the GRAS gene family in Brassica napus reveals their roles in root development and stress response. Planta 2019;250.
[17] Zhang S, Li X, Fan S, Zhou L, Wang Y. Overexpression of HcSCL13, a Halostachys caspica GRAS transcription factor, enhances plant growth and salt stress tolerance in transgenic Arabidopsis. Plant Physiol Biochem 2020;151.
[18] Bolle C. The role of GRAS proteins in plant signal transduction and development. Planta 2004;218:683–92.
[19] Sun X, Jones WT, Rikkerink EHA. GRAS proteins: the versatile roles of intrinsically disordered proteins in plant signalling. Biochem J 2012;442:1–12.
[20] Sun X, Xue B, Jones WT, Rikkerink E, Dunker AK, Uversky VN. A functionally required unfoldome from the plant kingdom: intrinsically disordered N-terminal domains of GRAS proteins are involved in molecular recognition during plant development. Plant Mol Biol 2011;77:205–23.
[21] Wang L, Ding X, Gao Y, Yang S. Genome-wide identification and characterization of GRAS genes in soybean (Glycine max). BMC Plant Biol 2020;20:415.
[22] Shan Z, Luo X, Wu M, Wei L, Fan Z, Zhu Y. Genome-wide identification and expression of GRAS gene family members in cassava. BMC Plant Biol 2020;20.
[23] Rui T, Han N, Hu Y, Wang L, Ren Z, Wang L. Genome-wide Identification and Expression Analysis of GRAS Genes in Cucumber, International Journal of. Horticulture 2020.
[24] To V-T, Shi Q, Zhang Y, Shi J, Shen C, Zhang D, et al. Genome-Wide Analysis of the GRAS Gene Family in Barley (Hordeum vulgare L.). Genes 2020;11:553.
[25] Mahesh H, Shirke MD, Singh S, Rajamani A, Hittalmani S, Wang G-L, Gowda M. Indica rice genome assembly, annotation and mining of blast disease resistance genes. BMC Genomics 2016;17.
[26] Philippe L, Berardini TZ, Li D, David S, Christopher W, Rajkumar S, et al. The Arabidopsis Information Resource (TAIR): improved gene annotation and new tools. Nucleic Acids Res 2012:1202–10.
[27] Zhang L, Li X, Ma B, Gao Q, Du H, Han Y, et al. The Tartary Buckwheat Genome Provides Insights into Rutin Biosynthesis and Abiotic Stress Tolerance. Molecular Plant 2017;10.
[28] Dohm J, Minoche A, Holtgräwe D, Capella-Gutierrez S, Zakrzewski F, Tafer H, et al. The genome of the recently domesticated crop plant sugar beet (Beta vulgaris). Nature 2013;505.
[29] Jarvis D, Ho YS, Lightfoot D, Schmöckel S, Li B, Borm T, et al. The genome of Chenopodium quinoa. Nature 2017;542:1–6.
[30] Yasui Y, Hirakawa H, Oikawa T, Toyoshima M, Matsuzaki C, Ueno M, et al. Draft genome sequence of an inbred line of Chenopodium quinoa, an allotetraploid crop with great environmental adaptability and outstanding nutritional properties. DNA Res 2016;23:dsw037.
[31] Mangelson H, Jarvis D, Mollinedo P, Rollano-Penaloza O, Palma V, Gomez-Pando L, et al. The genome of Chenopodium pallidicaule: An emerging Andean super grain. Appl Plant Sci 2019;7.
[32] Iorizzo M, Ellison S, Senalik D, Zeng P, Satapoomin P, Huang J, et al. A high-quality carrot genome assembly provides new insights into carotenoid accumulation and asterid genome evolution. Nat Genet 2016;48.
[33] Reyes-Chin-Wo S, Wang Z, Yang X, Kozik A, Arikit S, Song C, et al. Genome assembly with in vitro proximity ligation data and whole-genome triplication in lettuce. Nat Commun 2017;8:14953.
[34] Badouin H, Gouzy J, Grassa C, Murat F, Staton S, Cottret L, et al. The sunflower genome provides insights into oil metabolism, flowering and Asterid evolution. Nature 2017;546.
[35] Unver T, Wu Z, Sterck L, Turktas M, Lohaus R, Li Z, et al. Genome of wild olive and the evolution of oil biosynthesis. Proc Natl Acad Sci U S A 2017;114:E9413–22.
[36] Xu S, Brockmöller T, Navarro Quezada A, Kuhl H, Gase K, Ling Z, et al. Wild tobacco genomes reveal the evolution of nicotine biosynthesis. Proc Natl Acad Sci 2017;114:201700073.
[37] Xu X, Pan S, Cheng S, Zhang B, Mu D, Ni P, et al. Genome sequence and analysis of tuber crop potato. Nature 2011;475:189–95.
[38] Consortium TG. The tomato genome sequence provides insights into fleshy fruit evolution. Nature 2012.
[39] Huang S, Ding J, Deng D, Tang W, Liu Y. Draft genome of the kiwifruit Actinidia chinensis. Nat Commun 2013;4:2640.
[40] Filiault DL, Ballerini ES, Mandáková T, Akz G, Nordborg M. The Aquilegia genome provides insight into adaptive radiation and reveals an extraordinarily polymorphic chromosome with a unique history. eLife 2018;7.
[41] Material SO, Web S, Press H, York N, Nw A. The Amborella genome and the evolution of flowering plants. Science, 342. p. 1467.
[42] Van Aken O, Whelan J. Comparison of transcriptional changes to chloroplast and mitochondrial perturbations reveals common and specific responses in arabidopsis. Front Plant Sci 2012;3:281.
[43] Goda H, Sasaki E, Akiyama K, Maruyama-Nakashita A, Nakabayashi K, Li W, et al. The AtGenExpress hormone- and chemical-treatment data set: Experimental design, data evaluation, model data analysis, and data access. Plant J: Cell Mol Biol 2008;55:526–42.
[44] Clifton R, Lister R, Parker K, Sappl P, Elhafez D, Millar A, et al. Stress-Induced co-expression of alternative respiratory chain components in Arabidopsis thaliana. Plant Mol Biol 2005;58:193–212.
[45] Short E, North K, Roberts M, Hetherington A, Shirras A, McAinsh M. A stress-specific calcium signature regulating an ozone-responsive gene expression network in Arabidopsis. Plant J: Cell Mol Biol 2012;71:948–61.
[46] Kleine T, Kindgren P, Benedict C, Hendrickson L, Strand A. Genome-Wide Gene Expression Analysis Reveals a Critical Role for CRYPTOCHROME1 in the Response of Arabidopsis to High Irradiance. Plant Physiol 2007;144:1391–406.
[47] M. Krogh Jensen, P. Hagedorn, M. Torres-Zabala, M. Grant, J. Rung, D. Collinge, et al., Transcriptional regulation by an NAC (NAM-ATAF1,2-CUC2) transcription factor attenuates ABA signalling for efficient basal defence towards Blumeria graminis f. sp. hordei in Arabidopsis, Plant J: Cell Mol Biol 56 (2008) 867–880.
[48] Zipfel C, Kunze G, Chinchilla D, Caniard A, Jones J, Boller T, et al. Perception of the Bacterial PAMP EF-Tu by the Receptor EFR Restricts Agrobacterium-Mediated Transformation. Cell 2006;125:749–60.
[49] Nishimura M, Stein M, Hou B-H, Vogel J, Edwards H, Somerville S. Loss of a Callose Synthase Results in Salicylic Acid-Dependent Disease Resistance. Science (New York, N.Y.) 2003;301:969–72.
[50] McWhite C, Papoulas O, Drew K, Cox R, June V, Dong O, et al. A Pan-plant Protein Complex Map Reveals Deep Conservation and Novel Assemblies. Cell 2020;181.
[51] O'Malley R, Huang S-S, Song L, Lewsey M, Bartlett A, Nery J, et al. Cistrome and Epicistrome Features Shape the Regulatory DNA Landscape. Cell 2016;166:1598.
[52] Matasci N, Hung L-H, Yan Z, Carpenter E, Wickett N, Mirarab S, et al. Data access for the 1000 Plants (1KP) project. GigaScience 2014;3:17.
[53] Alex B. The Pfam protein families database: towards a more sustainable future. Nucleic Acids Res 2015;D1.
[54] ESR. HMMER web server: interactive sequence similarity searching. Nucl Acids Res (2011) suppl_2.
[55] Letunic I, Doerks T, Bork P. SMART 7: recent updates to the protein domain annotation resource. Nucleic Acids Res 2012;40.
[56] Finn R. The Pfam protein families database: Towards a more sustainable future. Nucleic Acids Res 2016;44:D279–85.
[57] Zdobnov E, Apweiler R. InterProScan. An integration platform for the signature-recognition methods in InterPro. Bioinformatics 2001;17:847–8.
[58] Emms D, Kelly S. OrthoFinder2: fast and accurate phylogenomic orthology analysis from gene sequences; 2018.
[59] Edgar R. MUSCLE: A multiple sequence alignment method with reduced time and space complexity. BMC Bioinf 2004;5:113.
[60] Kumar S, Stecher G, Tamura K. MEGA7: Molecular evolutionary genetics analysis version 7.0 for bigger datasets. Mol Biol Evolut 2016;33:msw054.
[61] Bailey T, Bodén M, Buske F, Frith M, Grant C, Clementi L, et al. MEME SUITE: tools for motif discovery and searching. Nucleic Acids Res 2009;37:W202–8.
[62] Marra MA. Circos: An information aesthetic for comparative genomics. Genome Res 2009;19:1639–45.
[63] Chen C, Rui X, Hao C, He Y. TBtools, a Toolkit for Biologists integrating various HTS-data handling tools with a user-friendly interface; 2018.
[64] Tang H, Wang X, Bowers J, Ming R, Alam M, Paterson A. Unraveling Ancient Hexaploidy Through Multiply-Aligned Angiosperm Gene Maps. Genome Res 2008;18:1944–54.
[65] Zhang Z, Li J, Zhao X-Q, Wang J, Wong G, Yu J. KaKs_Calculator: Calculating Ka and Ks Through Model Selection and Model Averaging. Genomics, Proteomics Bioinformatics 2006;4:259–63.
[66] Paterson AH. MCScanX: a toolkit for detection and evolutionary analysis of gene synteny and collinearity. Nucl Acids Res 40:e49.
[67] Song X, Li Y, Hou X. Genome-wide analysis of the AP2/ERF transcription factor superfamily in Chinese cabbage (Brassica rapa ssp. pekinensis). BMC Genomics 2013;14:573.
[68] Naggert JK. Defective carbohydrate metabolism in mice homozygous for the tubby mutation. Physiol Genomics 2006;27:131–40.
[69] Wang X. Hierarchically Aligning 10 Legume Genomes Establishes a Family-Level Genomics Platform. Plant Physiol 2017;174:284–300.
[70] Yarik. The arabidopsis information resource: Making and mining the "gold standard" annotated reference plant genome. Genesis: J Genetics Dev 2015.

[71] Akiyama K, Kurotani A, Iida K, Kuromori T, Shinozaki K, Sakurai T. RARGE II: An Integrated Phenotype Database of Arabidopsis Mutant Traits Using a Controlled Vocabulary. Plant Cell Physiol 2014;55:e4.
[72] Peterson M, Colosimo M. TreeViewJ: An application for viewing and analyzing phylogenetic trees. Source Code Biol Med 2007;2:7.
[73] Robles M. Blast2GO: a universal tool for annotation, visualization and analysis in functional genomics research. Bioinformatics 2005;21:3674–6.
[74] Ruiz Carrasco K, Antognoni F, Coulibaly A, Lizardi S, Covarrubias A, Martínez E et al. Variation in salinity tolerance of four lowland genotypes of quinoa (Chenopodium quinoa Willd.) as assessed by growth, physiological traits, and sodium transporter gene expression. Plant Physiol Biochem: PPB / Société française de physiologie végétale 2011;49:1333–41.
[75] Livak KJ, Schmittgen TD. Analysis of relative gene expression data using real-time quantitative PCR and the 2(-Delta Delta C(T)) Method. Methods 2012;25:402–8.
[76] Kolano B, Mccann J, Orzechowska M, Siwinska D, Temsch E, Weiss-Schneeweiss H. Molecular and cytogenetic evidence for an allotetraploid origin of Chenopodium quinoa and C. berlandieri (Amaranthaceae). Mol Phylogenet Evol 2016;100:109–23.
[77] Bolle C, Koncz C, Chua NH. PAT1, a new member of the GRAS family, is involved in phytochrome A signal transduction. Genes Dev 2000;14:1269–78.
[78] Gallagher K, Benfey P. Both the conserved GRAS domain and nuclear localization are required for SHORT-ROOT movement. Plant J: Cell Mol Biol 2008;57:785–97.
[79] Schmitz R, Schultz M, Urich M, Nery J, Pelizzola M, Libiger O, et al. Patterns of Population Epigenomic Diversity. Nature 2013;495.
[80] Hirsch S, Kim J, Muñoz A, Heckmann A, Downie J, Oldroyd G. GRAS Proteins Form a DNA Binding Complex to Induce Gene Expression during Nodulation Signaling in Medicago truncatula. Plant Cell 2009;21:545–57.
[81] Sun T-P. The molecular mechanism and evolution of the GA-GID1-DELLA signaling module in plants. Current Biol: CB 2011;21:R338–45.
[82] Cenci A, Rouard M. Evolutionary Analyses of GRAS Transcription Factors in Angiosperms. Front Plant Sci 2017;8.
[83] Cenci A, Guignon V, Roux N, Rouard M. Genomic analysis of NAC transcription factors in banana (Musa acuminata) and definition of NAC orthologous groups for monocots and dicots. Plant Mol Biol 2014;85:63–80.
[84] Tian C, Wan P, Sun S, Li J, Chen M. Genome-Wide Analysis of the GRAS Gene Family in Rice and Arabidopsis. Plant Mol Biol 2004;54:519–32.
[85] Lee MH, Kim B, Song SK, Heo JO, Yu NI, Lee SA, et al. Large-scale analysis of the GRAS gene family in Arabidopsis thaliana. Plant Mol Biol 2008;67:659–70.
[86] Song X-M, Liu T, Duan W, Ma Q-H, Ren J, Wang Z, et al. Genome-wide analysis of the GRAS gene family in Chinese cabbage (Brassica rapa ssp. Pekinensis). Genomics 2013;103.
[87] Yazaki J, Galli M, Kim A, Nito K, Aleman F, Chang K, et al. Mapping transcription factor interactome networks using HaloTag protein arrays. Proc Natl Acad Sci 2016;113:201603229.
[88] Eunkyoo O, Zhu JY, Bai MY, Augusto AR, Yu S, Wang ZY. Cell elongation is regulated through a central circuit of interacting transcription factors in the Arabidopsis hypocotyl 2014;3:e03031.
[89] Bai MY, Shang JX, Oh E, Fan M, Bai Y, Zentella R, et al. Brassinosteroid, gibberellin and phytochrome impinge on a common transcription module in Arabidopsis. Nat Cell Biol 2012;14:810–7.
[90] Feng S, Martinez C, Gusmaroli G, Wang Y, Zhou J, Wang F, et al. Coordinated regulation of Arabidopsis thaliana development by light and gibberellins. Nature 2008;451:475–9.
[91] Winkel B. It Takes a Garden. How Work on Diverse Plant Species Has Contributed to an Understanding of Flavonoid Metabolism. Plant Physiol 2002;127:1399–404.
[92] Pelletier M, Murrell J, Winkel B. Characterization of flavonol synthase and leucoanthocyanidin dioxygenase genes in Arabidopsis. Further evidence for differential regulation of "early" and "late" genes. Plant Physiol 1997;113:1437–45.
[93] Jeong ST, Goto-Yamamoto N, Kobayashi S, Esaka M. Effects of plant hormones and shading on the accumulation of anthocyanins and the expression of anthocyanin biosynthetic genes in grape berry skins. Plant Sci 2004;167:247–52.
[94] Kianersi F, Abdollahi M, Mirzaie-asl A, Dastan D, Rasheed F. Identification and tissue-specific expression of rutin biosynthetic pathway genes in Capparis spinosa elicited with salicylic acid and methyl jasmonate 2020.
[95] Mendoza D, Arias J, Cuaspud Caliz O, Ruiz O, Arias M. Methyl jasmonate/salicylic acid enhanced flavonoid production and change metabolites profile in Thevetia peruviana cell culture; 2018.